Reconsideration of Solvent Effects Calculated by Semiempirical Quantum Chemical Methods

Miroslaw Szafran,[1,2]* Mati M. Karelson,[3] Alan R. Katritzky,[1] Jacek Koput,[2] and Michael C. Zerner[1]

[1]Department of Chemistry, University of Florida, Gainesville, 32611, [2]Department of Chemistry, A. Mickiewicz Univerity, 60780 Poznan, Poland, and [3]Laboratory of Chemical Kinetics and Catalysis, Tartu University, Tartu 202400, Estonia

AM1 and PM3 semiempirical calculations are reported for the solvent effects on the tautomeric equilibria of 2-pyridone/2-hydroxypyridine and 4-pyridone/4-hydroxypyridine in the gas phase and solution. The solvent effects on the tautomeric equilibria were investigated by self-consistent reaction field (SCRF) theory implemented in the AMPAC and MOPAC program in two different ways: one in which all the solvent relaxation is included in the quantum mechanics and the total energy must be corrected for the solvent change in energy, method A; and a second in which the quantum mechanics directly includes this term, method B. The calculated (AM1, method A) tautomeric equilibrium constants (log K_l) for 2-pyridone in the gas phase, cyclohexane, chloroform, and acetonitrile are $-0.3, 0.3, 0.8$, and 1.3, respectively, in good agreement with the experimental data ($-0.4, 0.24, 0.78$, and 2.17, respectively). For 4-pyridone/4-hydroxypyridine differences between calculated log K_l for the gas phase, chloroform and acetonitrile ($-6.0, -2.6$, and -1.2, respectively) and experimental data ($< -1, 0.11$, and 0.66, respectively) are larger but the experimental values are also less certain. The experimental acetonitrile data are disturbed by specific interactions. An extension of the SCRF for aqueous solutions is reviewed. © 1993 by John Wiley & Sons, Inc.

INTRODUCTION

Interactions between solute and solvent molecules are responsible for variations of physical and chemical properties of the solute in going from the gas phase to the condensed phase (solution and/or solid state). Both classic and quantum mechanical approaches are in common use today to examine such interactions. In the classic approaches, molecular interactions are often divided into nonspecific (or physical, which is a sum of dispersion and electrostatic components) and specific (or chemical, represented by hydrogen bonding, charge–transfer, and strong dipole–dipole interactions). Classic concepts are well reviewed by Malecki.[1] In quantum chemical treatments, the interaction energy, ΔE, of a complex can be decomposed into five components: electrostatic (ES), polarization (PL), exchange repulsion (EX), charge transfer (CT), and dispersion (DISP).[2] Although only ΔE is measured, energy components provide extremely useful quantities that allow insight to be gained into the nature of the interaction in molecular complexes. Note, however, that the electrostatic, polarization, and dispersion terms in the two approaches have different meanings.

The effect of solvents on solute molecules may be categorized into specific and nonspecific classes as it is often possible to distinguish these two types of interactions by experiment.[1,3] Nonspecific interactions can arise from dispersion and electrostatic effects. In essence, the nonspecific influences are produced by electrostatic interactions between the charge distribution of the solute and solvent molecules and this can be described, for example, by a moment expansion such as that given by the Onsager reaction field theory.[4] Tapia and Goscinski[5] developed a quantum mechanical self-consistent reaction field (SCRF) theory based upon interacting dipole moments. Since then, this model has been applied to a number of problems with use of both semiempirical MO theory[6-11] and *ab initio* MO theory.[12] In these articles, somewhat different theoretical approaches were used and these differences require some explanation, one function of this article. A second aim of this article is to examine more systematically the performance of the two SCRF models being used. Note that several other methods that include solvent effects through SCRF techniques have been recently introduced.[2c,13,14]

REACTION FIELD THEORY

The nonspecific solvation energy consists of two main parts: induction and dispersion. Dispersion

forces belong to the most universal forces acting between molecules. These forces result from a correlation of the electron movements occurring in the solute with those of the solvent. The electrostatic interaction energy is usually larger and may be conveniently described by the Kirkwood[15] generalization of the Onsager reaction field model.[4] In this model, the solute is placed in a cavity (spherical or ellipsoidal) immersed in a continuous medium characterized by a dielectric constant, ϵ. The electric field of the solute molecule polarizes the surrounding media, and this new field reacts back on the solute molecular system. In the quantum mechanical approach,[5,6] the solvent effect is taken as an additional term, H_1, in the Hamiltonian of the isolated molecule (solute), H_0, obtained from the system energy (assuming only a dipole interaction; see ref. 6):

$$E = E_0 - 0.5\mathbf{R}\langle\Psi|\mu|\Psi\rangle \tag{1}$$

where μ is the electric dipole moment operator and Ψ is the molecular wave function. The reaction (electric) field operator, $\mathbf{R}$, is proportional to the solute dipole moment, μ[4,7]:

$$\mathbf{R} = \mathbf{g}\mu \tag{2}$$

The coupling tensor, $\mathbf{g}$, is the Onsager factor,[4] which gives the strength of the reaction field and depends upon the dielectric constant of the medium, ϵ, and, in the simplest case, upon the radius of the spherical cavity, a_0.

$$\mathbf{g} = ((2(\epsilon - 1))/((2\epsilon + 1)a_0^3))\mathbf{1} \tag{3}$$

After variations, the Schrödinger equation for a solute is then given by eq. (4).

$$(H_0 - \lambda\mu\mathbf{g}\langle\Psi|\mu|\Psi\rangle)\Psi = E|\Psi\rangle \tag{4}$$

The parameter λ is dependent upon the constraints of the variation. If normality of the wave function is the only constraint $((\langle\Psi|\Psi\rangle = 1)$ $\lambda = 1$, and this is equivalent to considering the solvent as an isothermal bath. If an additional constraint is imposed that eq. (1) is obtained after variation

$$\langle\Psi|H|\Psi\rangle = \langle\Psi|H_0 + H_1|\Psi\rangle$$
$$= \langle\Psi|H_0|\Psi\rangle - 0.5g\langle\Psi|\mu|\Psi\rangle^2 \tag{5}$$

Then, $\lambda = 0.5$ and, in this sense, the solvent is included in the variation. The Schrödinger eq. (1) can be solved within the framework of the standard Hartree–Fock theory, leading to

$$(F_0 - \lambda\mu\mathbf{g}\langle\Psi|\mu|\Psi\rangle)|\Phi_i\rangle = \epsilon_i|\Phi_i\rangle \tag{6}$$

where F_0 is the effective one-electron Fock operator, Φ_i is a molecular orbital, and ϵ_i is a molecular orbital energy. The total energy for method A, which is given when $\lambda = 1$, is

$$E_t = E_{qm} + 0.5\mu\mathbf{R} = \langle\Psi|H|\Psi\rangle + 0.5g\langle\Psi|\mu|\Psi\rangle^2$$

$$= \langle\Psi|H_0|\Psi\rangle - 0.5g\langle\Psi|\mu|\Psi\rangle^2 \tag{7}$$

Note that the solvent "cost" energy, $0.5g\langle\Psi|\mu|\Psi\rangle^2$, must be added back to that obtained from the quantum mechanics to generate eq. (1). Method B is defined when $\lambda = 0.5$. In this case, the quantum mechanical energy yields directly the total energy as shown in eq. (5). Method A is the more traditional one and its derivation is rather straightforward.[5] Method B should yield similar results for reasonable cavity radius as the total energy expressions for a given g are the same and has the advantage of yielding analytic derivatives with respect to nuclear displacement that are required for geometry optimization in a rather easy fashion.[6,10] Method A requires a numerical differentiation, or the solution of the coupled-perturbed Hartree–Fock equations, if analytic equations are to be obtained.

In both methods A and B, the coupling tensor g is taken as a parameter. From a comparison of eq. (6), it is clear that both methods would lead to the same molecular wave functions if the geometry is the same and if assumed values of the coupling tensor differ by a factor of 0.5, i.e.

$$a_0(\text{method A}) = 2^{1/3}a_0(\text{method B}) \tag{8}$$

The total energies, however (and thus also the geometry), will not be similar for, as we discussed previously, eqs. (5) and (7) should yield similar results for the *same* a_0.

The SCRF Hamiltonian is an unbounded operator, and the stability of its solution will depend upon the size of the H_1 relation to H_0. For a given a_0, the wave function obtained from eq. (7) will be different but the total energies should be similar for well-behaved H_1. As a_0 decreases, we might expect this equivalence in models to be destroyed and both models to yield unphysical results.

Methods A and B have been implemented into the AMPAC (v.2.1) and MOPAC (v.5.0) program packages and the resulting molecular orbital problem is solved iteratively as in refs. 9(b) and 10. Method A reproduces exactly the Tapia and Silvi[6] data. In ref. 11, calculations are done with method A and in refs. 9 and 10 with method B. Note that in refs. 9(a)–(e) λ is omitted ($\lambda = 1$) but the calculations have been done when $\lambda = 0.5$.

ESTIMATION OF CAVITY RADIUS

The choice of cavity radius has been the subject of much discussion.[1,12b,13,16] The simplest approach is to calculate the radius from the experimental solute molecular volume ($V_m = $ mol.wt./density)

$$a_0 = (3V_m/(4\pi N))^{1/3} \cong 0.734\ V_m^{1/3} \tag{9}$$

where N is Avogadro's number. The molar volume can also be obtained from its refractivity.[17] Another approach is to estimate a_0 from the molecule's great-

est dimension.[12b] In this approach, the diameter of the molecule is calculated from the greatest inter-molecular distance (in the direction of the dipole moment) and by adding the van der Waals radii[18] of the two atoms involved. Wibert et al.[12b] proposed to use eq. (9) to determine the a_0 value and then add 0.5 Å to the final value. The constant term (0.5 Å) is added to account for the van der Waals radii of the surrounding solvent molecules.

The cavity radius of hydroxypyridines/pyridone systems estimated from the molar volume of meth-ylpyridines [eq. (9)] and adding 0.5 Å to account for the nearest approach of solvent molecules gives $a_0 = 3.38 + 0.5 = 3.88$ Å. Using the greatest dimension and adding the van der Waals radii of the peripheral atoms as described above leads to $a_0 = 3.95$ and 3.88 Å, respectively, for hydroxypyridines and pyridones. The above values are comparable with $a_0 = 3.80$ Å calculated by Wibert et al.[12d] for 2-hydroxypyridine/2-pyridone system. In this article, we use $a_0 = 3.80$ Å, unless mentioned otherwise, to compare our results with the *ab initio* molecular structures.[12d]

Most organic molecules are not spherical. Thus, Rivail et al.[16] proposed a three-axes ellipsoidal model that better describes the shape of molecules. However, this modification does not essentially influence the results,[7b,19] whereas it introduces the ratio of ellipsoidal axes as an additional parameter.

The quantity $(\epsilon - 1)/(2\epsilon + 1)$ that enters into g, eq. (3), tends to the value of 0.5 when $\epsilon \to \infty$ (Fig. 1) and thus the Onsager reaction field will produce similar results for solvents with $\epsilon \geq 15$. Yet, differences between such solvents can be large due to specific solute–solvent interactions. This has been examined in some detail in refs. 6 and 20. For water ($\epsilon = 78.4$) solutions, it has been shown that a su-permolecule of solute and bonded solvent mole-
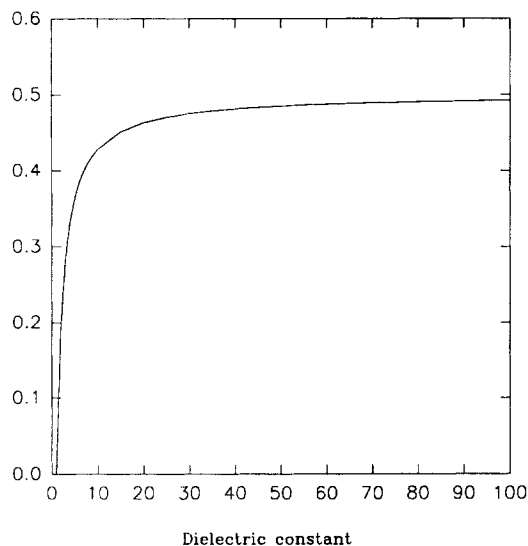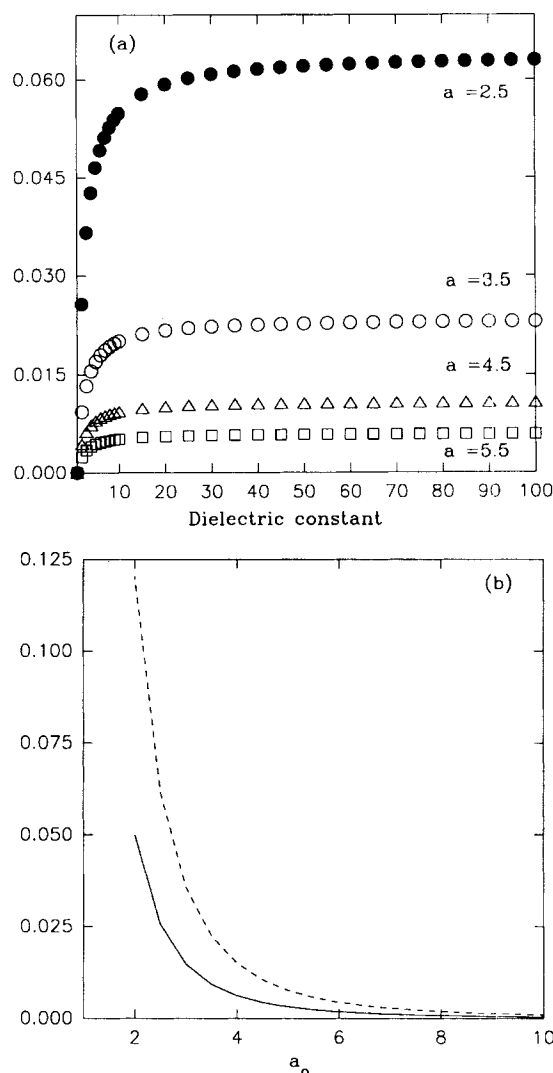

Figure 2. (a). Plot of $(\epsilon - 1)/(2\epsilon + 1)$ vs. dielectric constant (ϵ) for different spherical cavity radius (a_0). (b). Plot of $(\epsilon - 1)/(2\epsilon + 1)$ vs. spherical cavity radius (a_0) for $\epsilon = 2$ (———) and $\epsilon = 40$ (– – –).

cules, all embedded in an Onsager cavity, yields reliable results.[1]

Figure 2 shows variations of g with ϵ and a_0.

The properties of water (and many speculations about the structure of its liquid state) are documented in the enormous literature.[21] It is also well documented that water forms hydrogen bonding complexes with polar molecules and ions in organic solvents and in the vapor phase.[22] Thus, in aqueous solutions specific solvent effects such as hydrogen bonding and donor–acceptor interactions cannot be neglected.

RESULTS AND DISCUSSION

All calculations were run with the selection FULSCF and PRECISE key words.

In Table I, we report the heats of formation of 2-pyridone and 2-hydroxypyridine calculated by

Figure 1. Plot of $(\epsilon - 1)/(2\epsilon + 1)$ vs. ϵ.

Table I. Calculated AM1 and PM3 heats of formation (kcal mol^{-1}) of 2-pyridone and 2-hydroxypyridine in the gas phase and solutions.

	2-Pyridone				2-OH-pyridine			
	AM1		PM3		AM1		PM3	
ϵ	A	B	A	B	A	B	A	B
1	−11.3	−11.3	−15.7	−15.6	−11.8	−11.8	−18.1	−18.1
2	−12.3	−12.2	−16.4	−16.3	−11.9	−11.9	−18.2	−18.2
4.81	−13.1	−12.9	−17.2	−17.0	−12.0	−12.0	−18.3	−18.2
35.9	−13.9	−13.6	−17.9	−17.6	−12.1	−12.0	−18.4	−18.3
78.4	−14.0	−13.6	−18.0	−17.7	−12.2	−12.0	−18.4	−18.3
1[a]	−78.9	−78.9	−73.7	−73.7	−75.9	−75.9	−74.2	−74.2
78.4[a]	−83.5	−81.5	−78.5	−76.9	−77.8	−77.0	−76.6	−75.8

Cavity radii, $a_0 = 3.8$ Å.
[a]Hydrate.

Table II. Calculated AM1 and PM3 dipole moments (D) of 2-pyridone and 2-hydroxypyridine in the gas phase and solutions.

	2-Pyridone				2-OH-pyridine			
	AM1		PM3		AM1		PM3	
ϵ	A	B	A	B	A	B	A	B
1	3.92	3.92	3.69	3.69	1.38	1.38	1.24	1.24
2	4.29	4.14	4.03	3.91	1.50	1.46	1.35	1.31
4.81	4.62	4.35	4.34	4.05	1.61	1.52	1.43	1.35
35.9	4.94	4.49	4.63	4.24	1.71	1.59	1.51	1.41
78.4	4.97	4.52	4.66	4.25	1.72	1.59	1.52	1.42
1[a]	3.36	3.36	3.23	3.23	2.80	2.80	3.19	3.19
78.4[a]	8.30	7.51	8.02	7.08	3.75	3.44	4.26	3.71

Cavity radii, $a_0 = 3.8$ Å.
[a]Hydrate.

the AM1 and PM3 parametrization schemes of the MNDO model Hamiltonians of Dewar and collaborators[23] and Stewart.[24] Models A and B yield results in amazingly good agreement with one another considering that the dipole moments obtained from the different Fock operators of eq. (6) can be quite different, as shown in Table II. Included in these tables are the results for a monohydrate calculated quantum mechanically as a supermolecule embedded in the dielectric media. Tables III and IV report similar results for the 4-pyridone/4-hydroxypyridine

system. In all cases, the energies obtained from model A are slightly lower than those obtained from model B, as might be expected from the greater interaction between solute and solvent in model A. These differences, again as expected, increase with increasing dielectric constant.

In Table V, we report the results of calculations for the log K_t for the 2-pyridone $\rightleftarrows$ 2-hydroxypyridine equilibrium. For this, we use the same a_0 and note that both models A and B make similar predictions. The tautomeric equilibrium constants have been determined by UV spectroscopic experiments.[25] These values correspond to the free energy $\Delta G = \Delta H - T\Delta S = -2.303RT \log K_t$. Recently, Wiberg et al.[12d] have shown that in the case of 2-pyridone contribution of $-T\Delta S$ to the free energy varies from 0.13 to 0.08 kcal/mol. Thus, the logarithm of the tautomeric equilibrium should be approximately linear with the corresponding enthalpy change:

$$\log K_t \cong -\Delta H/2.303RT \cong -\Delta H/1.364 \quad (10)$$

The results from the AM1 Hamiltonian are in good accord with experimental and those from ab initio calculations, those from the PM3 model being somewhat worse. Results for acetonitrile ($\epsilon = 35.9$) and from aqueous solution ($\epsilon = 78.4$) do not reflect the

Table III. Calculated AM1 and PM3 heats of formation (kcal mol^{-1}) of 4-pyridone and 4-hydroxypyridine in the gas phase and solutions.

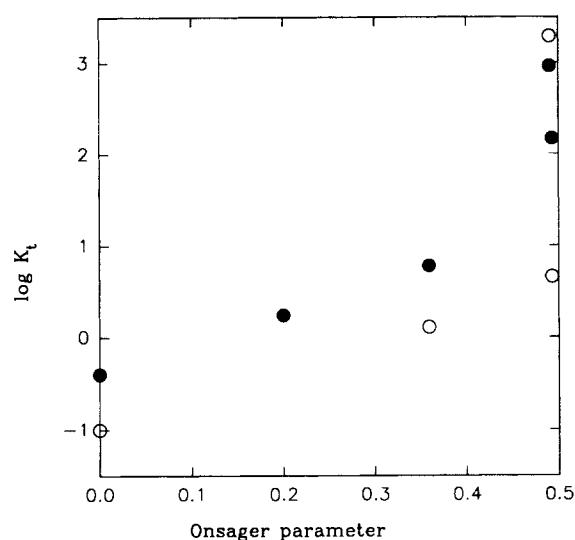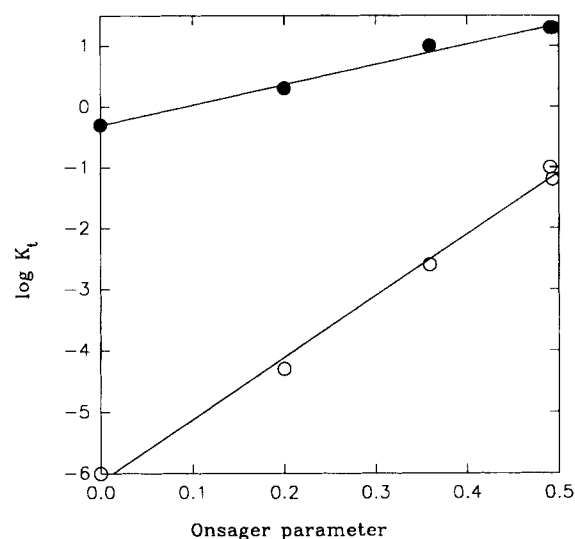|	4-Pyridone				4-OH-pyridine			
	AM1		PM3		AM1		PM3	
ϵ	A	B	A	B	A	B	A	B
1	−4.5	−4.5	−6.6	−6.6	−12.7	−12.7	−15.2	−15.2
2	−7.2	−6.8	−9.0	−8.7	−13.1	−12.9	−15.7	−15.5
4.81	−9.8	−8.9	−11.3	−10.6	−13.4	−13.1	−16.1	−15.7
35.9	−12.1	−10.6	−13.4	−12.2	−13.7	−13.3	−16.4	−15.9
78.4	−12.3	−10.9	−13.6	−12.3	−13.7	−13.3	−16.5	−15.9
1[a]	−134.1	−134.1	−122.2	−122.2	−138.5	−138.5	−129.2	−129.2
78.4[a]	−161.6	−151.0	−149.6	−138.9	−148.6	−144.5	−141.6	−137.2

Cavity radii, $a_0 = 3.8$ Å.
[a]Dihydrates.

Table IV. Calculated AM1 and PM3 dipole moments (D) of 4-pyridone and 4-hydroxypyridine in the gas phase and solutions.

| | 4-Pyridone | | | | 4-OH-pyridine | | | |
| | AM1 | | PM3 | | AM1 | | PM3 | |
ϵ	A	B	A	B	A	B	A	B
1	6.29	6.29	6.01	6.01	1.98	1.98	2.16	2.16
2	7.00	6.66	6.70	6.41	2.14	2.07	2.33	2.27
4.81	7.70	7.00	7.38	6.77	2.28	2.15	2.48	2.35
35.9	8.34	7.28	8.01	7.07	2.41	2.21	2.62	2.42
78.4	8.39	7.31	8.07	7.16	2.42	2.21	2.63	2.42
1[a]	9.59	9.59	6.26	6.26	5.88	5.88	7.01	7.01
78.4[a]	16.17	13.10	16.87	13.07	8.57	7.31	9.76	8.25

Cavity radii, a_0 = 3.8 Å.
[a]Dihydrates.

Figure 3. Plot of experimental $\log K_t$ vs. $(\epsilon - 1)/(2\epsilon + 1)$; 2-pyridone (●) and 4-pyridone (○).

experimental values as accurately as those obtained for smaller dielectric solvents. These media, however, might be expected to have specific interactions with the solute molecules. Figures 3 and 4 show experimental and AM1 values of $\log K_t$ plotted vs. $(\epsilon - 1)/(2\epsilon + 1)$, respectively. In the case of experimental data, a nonlinear curve is obtained and water is certainly not on the curve, a consequence of specific interactions that take place in aqueous solutions.[6,21] Included in Table V are also the results from a calculation that treats one water molecule specifically along with the solute and the entire supermolecule embedded in the reaction field. This results in a predicted $\log K_t$ from the AM1 calculations of 3.3, compared to the experimental value of 2.96. Again, the AM1 value is better than that obtained from the PM3 parametrization, 0.9. In Table VI, we report the results we obtain for the $\log K_t$ for the 4-pyridone/4-hydroxypyridine system. The differences between models A and B obtained here are somewhat greater than those obtained for the 2-pyridone/2-hydroxypyridine system, as might be expected from the larger differences in dipole moments given in Table IV. Although all the methods make qualitatively correct predictions for this system, none is particularly good when compared with the

Figure 4. Plot of the AM1 $\log K_t$ vs. $(\epsilon - 1)/(2\epsilon + 1)$; 2-pyridone (●) and 4-pyridone (○).

Table V. Calculated relative energies (kcal/mol) and tautomeric equilibrium constants for [NH]/[OH] for 2-pyridone and 2-hydroxypyridine in the gas phase and solutions.

| | Relative stability | | | | $\log K_t$ | | | | | |
| | AM1 | | PM3 | | AM1 | | PM3 | | 6-31G** | Exp. |
ϵ^a	A	B	A	B	A	B	A	B	(Ref. 12d)	(ref. 25)
1	0.5	0.5	2.5	2.5	-0.3	-0.3	-1.8	-1.8	-0.5	-0.4
2	-0.4	-0.3	1.8	1.8	0.3	0.2	-1.3	-1.3	0.3	0.24
4.81	-1.1	-1.0	1.1	1.2	0.8	0.7	-0.8	-0.9		0.78
35.9	-1.8	-1.5	0.5	0.7	1.3	1.1	-0.4	-0.5	1.7	2.17
78.4	-1.8	-1.6	0.4	0.6	1.3	1.2	-0.3	-0.4		2.96
1[b]	-3.0	-3.0	0.5	0.5	2.2	2.2	-0.3	-0.3		
78.4[b]	-5.7	-4.5	-1.9	-1.2	4.2	3.3	1.4	0.9		2.96

Cavity radii, a_0 = 3.8 Å.
[a]ϵ = 2 (cyclohexane); ϵ = 4.81 (chloroform); ϵ = 35.9 (acetonitrile); ϵ = 78.4 (water).
[b]Hydrate.

Table VI. Calculated relative energies (kcal/mol) and tautomeric equilibrium constants for [NH]/[OH] for 4-pyridone and 4-hydroxypyridine in the gas phase and solutions.

| | Relative stability | | | | log K_t | | | | |
| | AM1 | | PM3 | | AM1 | | PM3 | | Exp. |
ϵ	A	B	A	B	A	B	A	B	(ref. 25)
1	8.2	8.2	8.5	8.5	−6.0	−6.0	−6.3	−6.3	< −1
2	5.9	6.1	6.7	6.8	−4.3	−4.5	−4.9	−5.0	
4.81	3.6	4.2	4.8	5.1	−2.6	−3.1	−3.5	−3.8	0.11
35.9	1.6	2.7	3.0	3.7	−1.2	−1.9	−2.2	−2.7	0.66
78.4	1.4	2.4	2.9	3.6	−1.0	−1.8	−2.1	−2.6	3.29
1[a]	4.4	4.4	7.0	7.0	−3.2	−3.2	−5.1	−5.1	
78.4[a]	−13.0	−6.5	−8.0	−1.7	9.5	4.7	5.9	1.2	3.29

Cavity radii, $a_0 = 3.8$ Å.
[a]Dihydrates.

experimental values. Again, the AM1 method seems somewhat more accurate in reproducing the experimental values than the PM3 model.

Empirical solvent parameters describe both non-specific and specific interactions, and hence a plot of the log K_t vs. the Kossower Z parameter is a straight line (see ref. 25a). Some deviation is also observed for acetonitrile, perhaps a consequence of strong dipole–dipole interactions.[26]

In Tables VII and VIII, we report the calculated dipole moments obtained by models A and B when the a_0 value that enters the Fock operator scales as shown in eq. (8). These values would be identical as discussed in the text if the geometries were the same, but they are not as the total energies obtained from

Table VII. Calculated AM1 and PM3 dipole moments (D) of 2-pyridone and 2-hydroxypyridine in the gas phase and solutions.

| | 2-Pyridone | | | | 2-OH-pyridine | | | |
| | AM1 | | PM3 | | AM1 | | PM3 | |
ϵ	A	B	A	B	A	B	A	B
1	3.92	3.92	3.69	3.69	1.38	1.38	1.24	1.24
2	4.29	4.40	4.03	4.09	1.50	1.55	1.35	1.36
4.81	4.62	4.78	4.34	4.61	1.61	1.66	1.43	1.52
35.9	4.94	5.13	4.63	5.07	1.71	1.77	1.51	1.65
78.4	4.97	5.17	4.66	5.11	1.72	1.78	1.52	1.65

Cavity radii, $a_0 = 3.8$ Å (method A) and $a_0 = 3.016$ Å (method B).

Table VIII. Calculated AM1 and PM3 dipole moments (D) of 4-pyridone and 4-hydroxypyridine in the gas phase and solutions.

| | 4-Pyridone | | | | 4-OH-pyridine | | | |
| | AM1 | | PM3 | | AM1 | | PM3 | |
ϵ	A	B	A	B	A	B	A	B
1	6.29	6.29	6.01	6.01	1.98	1.98	2.16	2.16
2	7.00	7.19	6.70	6.85	2.14	2.19	2.33	2.38
4.81	7.70	7.89	7.38	7.88	2.28	2.35	2.48	2.59
35.9	8.34	8.69	8.01	8.68	2.41	2.5	2.62	2.79
78.4	8.39	8.77	8.07	8.75	2.42	2.51	2.63	2.79

Cavity radii, $a_0 = 3.8$ Å (method A) and $a_0 = 3.016$ Å (method B).
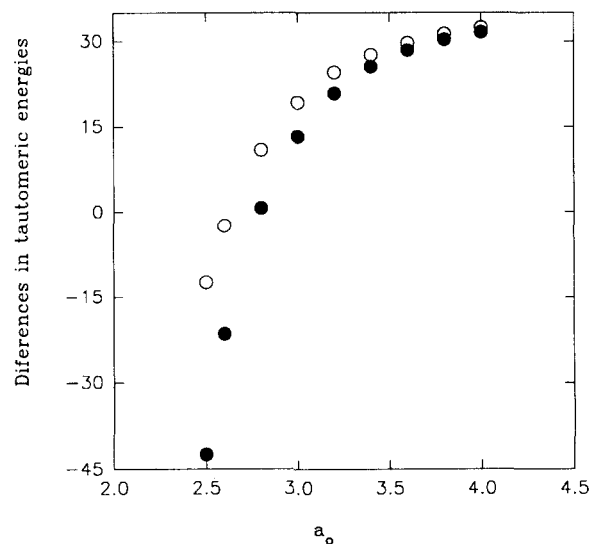
Figure 5. Plot of the calculated energy difference (kcal/mol) of 2H,4-oxo-pyrazole and 5H,4-oxo-pyrazole vs. cavity radius, a_0; method A (●) and method B (○).

models A and B are not. As seen in these tables, values are remarkably similar, suggesting geometric predictions are not different for models A and B.

In Figure 5, we plot the calculated differences in energies of 2H,4-oxo-pyrazole and 5H,4-oxo-pyrazole as a function of a_0. Clearly, model A becomes unstable before model B, a consequence of the greater effect this parameter has on the Fock equations of model A. Some care must be shown with the choice of cavity radius, but as we have shown for reasonable radii both models give similar results. Model B has the advantage in that it is relatively easy to calculate gradients of the energy with respect to nuclear coordinates, a requirement for rapid geometry searches.

CONCLUSIONS

Several important points emerge from this study:

1. The solvent effects on the tautomeric equilibria of 2- and 4-pyridones are satisfactorily repro-

duced by the AM1 method. The calculated tautomeric equilibrium constants for the gas phase, cyclohexane, and chloroform are in good agreement with the experimental data.

2. Onsager's reaction field theory appears to be a promising approach to examine the nonspecific electrostatic solute–solvent interaction. The separation of nonspecific and specific interactions in experimental measurements is difficult or impossible; hence, the specific interactions of solute with solvent distinctly affect an effective value of equilibrium constants. In these cases, a supermolecule approach, with one or more solvent molecules bound to the solute and the ensemble embedded in the dielectric continuum, seems successful.

3. We examined two plausible SCRF models. For a reasonable cavity radius, both theories seem successful, yielding similar results. The more successful model will require further testing, especially considering cavity volumes from fixed anzats, such as from eq. (9).

References

1. J. Malecki, In *Molecular Interactions*, Vol. 3, H. Ratajczak and W.J. Orville-Thomas, Eds. Wiley, Chichester, UK, 1982, p. 183.

2. (a) K. Morokuma, *Acc. Chem. Res.*, **10**, 294 (1977); (b) P.A. Kollman, *Acc. Chem. Res.*, **10**, 365 (1977); (c) J. Tomasi, In *Molecular Interactions*, Vol. 3, H. Ratajczak and W.J. Orville-Thomas, Eds. Wiley, Chichester, UK, 1982, p. 119.

3. C. Reichardt, *Solvents and Solvent Effects in Organic Chemistry*, Verlag Chemie, Weinheim, 1988.

4. L. Onsager, *J. Am. Chem. Soc.*, **58**, 1486 (1936).

5. O. Tapia and O. Goscinski, *Mol. Phys.*, **29**, 1653 (1975).

6. M.M. Karelson and M.C. Zerner, *J. Phys. Chem.*, **96**, 6949 (1992).

7. C.J.F. Böttcher and P. Bordewijk, *Theory of Electric Polarization*, Elsevier, Amsterdam, 1978.

8. O. Tapia and B. Silvi, *J. Phys. Chem.*, **84**, 2646 (1980).

9. (a) M.M. Karelson, A.R. Katritzky, M. Szafran, and M.C. Zerner, *J. Org. Chem.*, **54**, 6030 (1989); (b) M.M. Karelson, T. Tamm, A.R. Katritzky, S.J. Cato, and M.C. Zerner, *Tetrahedron Comp. Meth.*, **2**, 295 (1989); (c) M.M. Karelson, A.R. Katritzky, M. Szafran, and M.C.

Zerner, *J. Chem. Soc. Perkin Trans. II*, 195 (1990); (d) M.M. Karelson, T. Tamm, A.R. Katritzky, M. Szafran, and M.C. Zerner, *Int. J. Quantum Chem.*, **37**, 1 (1990); (e) M.M. Karleson, A.R. Katritzky, and M.C. Zerner, *J. Org. Chem.*, **56**, 134 (1991).

10. (a) H.S. Rzepa, M. Yin Yi, M.M. Karelson, and M.C. Zerner, *J. Chem. Soc. Perkin Trans. II*, 635 (1991); (b) H.S. Rzepa and M. Yin Yi, *J. Chem. Soc. Perkin Trans. II*, 531 (1991).

11. Z. Dega-Szafran, M. Gdaniec, M. Grundwald-Wyspianska, Z. Kosturkiewicz, J. Koput, P. Krzyzanowski, and M. Szafran. *J. Mol. Struct.*, **270**, 99 (1992).

12. (a) M.M. Karelson, A.R. Katritzky, and M.C. Zerner, *Int. J. Quantum Chem. Symp.*, **20**, 521 (1986); (b) M. Wah Wong, M.J. Frisch, and K.B. Wiberg, *J. Am. Chem. Soc.*, **113**, 4776 (1991); (c) M. Wah Wong, K.B. Wiberg, and M.J. Frisch, *J. Am. Chem. Soc.*, **114**, 523 (1992); (d) M. Wah Wong, K.B. Wiberg, and M.J. Frisch, *J. Am. Chem. Soc.*, **114**, 1645 (1992).

13. O. Tapia, In *Molecular Interactions*, Vol. 3, H. Ratajczak and W.J. Orville-Thomas, Eds. Wiley, Chichester, UK, 1982, p. 47.

14. K.V. Mikkelsen, H. Agren, H.J.A. Jensen, and T. Helgaker, *J. Phys. Chem.*, **89**, 3086 (1988).

15. (a) J.G. Kirkwood, *J. Chem. Phys.*, **2**, 351 (1934); (b) J.G. Kirkwood and F.H. Westheimer, *J. Chem. Phys.*, **6**, 506 (1938).

16. J.L. Rivail, B. Terryn, D. Rinaldi, and M.F. Ruiz-Lopez, *J. Mol. Struct. (THEOCHEM)*, **120**, 387 (1985).

17. (a) R.J.W. Le Fèvre, *Adv. Phys. Org. Chem.*, **3**, 1 (1965); (b) S.S. Batsanov, *Refractometry and Chemical Structure*, D. Van Nostrand, Princeton, NJ, 1966.

18. A. Bondi, *J. Phys. Chem.*, **68**, 441 (1964).

19. J.M. Thiébaut, J.L. Rivail, and J.L. Greffe, *J. Chem. Soc. Faraday Trans. II*, **72**, 2024 (1976).

20. M.M. Karelson and M.C. Zerner, *J. Am. Chem. Soc.*, **112**, 9405 (1990).

21. (a) F. Franks, Ed., *Water, A Comprehensive Treatise*, Vols. 1–5. Plenum Press, New York, 1972–1975; (b) C. Tanford, *The Hydrophobic Effect*, Wiley, New York, 1973; (c) R.L. Kay, *The Physical Chemistry of Aqueous Solutions*, Plenum, New York, 1973.

22. (a) S.D. Christian, A.A. Taha, and B.W. Gash, *Q. Rev. Chem. Soc.*, **24**, 20 (1970); (b) E.M. Arnett, B. Chawla, and N.J. Hornung, *J. Solution Chem.*, **6**, 781 (1977); (c) E.M. Arnett, *J. Educ. Chem.*, **62**, 385 (1985).

23. M.J.S. Dewar, E.G. Zoebisch, E.F. Healy, and J.J.P. Stewart, *J. Am. Chem. Soc.*, **107**, 3902 (1985).

24. J.J.P. Stewart, *J. Comp. Chem.*, **10**, 209, 221 (1989).

25. (a) J. Frank and A.R. Katritzky, *J. Chem. Soc. Perkin Trans. II*, 1428 (1976); (b) P. Beak, *Acc. Chem. Res.*, **10**, 186 (1977).

26. (a) C.D. Ritchie, B.A. Bierl, and R.J. Honour, *J. Am. Chem. Soc.*, **84**, 4687 (1962); (b) C.D. Ritchie and A.L. Pratt, *J. Phys. Chem.*, **67**, 2498 (1963); (c) C.D. Ritchie and A.L. Pratt, *J. Am. Chem. Soc.*, **86**, 1571 (1964).